A Mutant Hepatitis B Virus Core Protein Mimics Inhibitors of Icosahedral Capsid Self-Assembly[†]

Christina R. Bourne,[‡,§] Sarah P. Katen,[||] Matthew R. Fulz,[‡] Charles Packianathan,[||] and Adam Zlotnick*[,‡,||]

Department of Biochemistry and Molecular Biology, University of Oklahoma Health Sciences Center, Oklahoma City, Oklahoma 73104, and Department of Biology, Indiana University, Bloomington, Indiana 47405

Received September 23, 2008; Revised Manuscript Received January 5, 2009

ABSTRACT: Understanding self-assembly of icosahedral virus capsids is critical to developing assembly directed antiviral approaches and will also contribute to the development of self-assembling nanostructures. One approach to controlling assembly would be through the use of assembly inhibitors. Here we use Cp149, the assembly domain of the hepatitis B virus capsid protein, together with an assembly defective mutant, Cp149-Y132A, to examine the limits of the efficacy of assembly inhibitors. By itself, Cp149-Y132A will not form capsids. However, Cp-Y132A will coassemble with the wild-type protein on the basis of light scattering and size exclusion chromatography. The resulting capsids appear to be indistinguishable from normal capsids. However, coassembled capsids are more fragile, with disassembly observed by chromatography under mildly destabilizing conditions. The relative persistence of capsids assembled under conditions where association energy is weak compared to the fragility of those where association is strong suggests a mechanism of "thermodynamic editing" that allows replacement of defective proteins in a weakly associated complex. There is fine line between weak assembly, where assembly defective protein is edited from a growing capsid, and relatively strong assembly, where assembly defective subunits may dramatically compromise virus stability. Thus, attempts to control virus self-assembly (with small molecules or defective proteins) must take into account the competing process of thermodynamic editing.

Viruses have a long history as pathogens (see ref *1* and references therein) and a much shorter history as tools for the development of nanostructures (*2*−*8*). Biologically, virus assembly requires high fidelity and rapid kinetics. Virus assembly is a paradigm for nanostructure self-assembly. Controlling virus assembly therefore has value for development of new classes of antiviral agents and for developing viruses as platforms for nanotechnology.

The object of this study, hepatitis B virus (HBV),[1] is an unusually serious public health problem as a major contributing factor to cirrhosis and hepatocellular carcinoma that chronically infects approximately 400 million individuals (*9*). HBV is an enveloped DNA virus with an icosahedral core. The protein shell of HBV's core, the capsid, is a self-assembling complex of 120 core protein homodimers (*10, 11*). In vivo, the nucleoprotein core is critical to the virus life cycle (*9, 12*−*15*). In vitro, empty capsids can be recapitulated by the 149-residue core protein assembly domain (Cp149) (*16*). The interdimer contacts that form a capsid are compact, though not tightly packed, and dominated by hydrophobic residues (*17, 18*). Small molecules that occupy gaps at this interface are able to strengthen the interdimer association energy and divert assembly from its normal path (*19, 20*). HBV assembly has been characterized in detail with the aid of model-based analyses specific for icosahedral assembly (*21, 22*). There is a well-defined nucleation step, formation of a trimer of homodimers, which is critical for avoiding kinetic traps (*23*). The individual interdimer contacts are weak, though globally they result in a stable structure; the pairwise association energy is strengthened from −3.1 to −4.1 kcal/mol as the temperature and ionic strength increase (*24*). Even under conditions where they are nominally unstable, HBV capsids can persist due to hysteresis to dissociation (*25*). These characteristics—nucleated assembly, weak interaction energy, and hysteresis—may be general to assembly of all virus-like particles (*7, 23, 26*).

In general, virus capsid assembly can be disrupted by inappropriately enhancing (*19, 27*), misdirecting, distorting (*28, 29*), or inhibiting association (*29*−*32*). We hypothesize that there are two modes of action for assembly inhibitors. They can slow or altogether prevent the bound subunit from assembling; such an inhibitor will be required in great molar excess as an antiviral. Alternatively, an inhibitor that poisons further assembly by its association with a growing capsid can have a more far-reaching effect. In

[†] This work was supported by NIH Grants to A.Z. and by a Mary Horton-American Cancer Society Fellowship to C.R.B.

* To whom correspondence should be addressed: Department of Biology, Indiana University, 212 S. Hawthorne Dr., Simon Hall 220D, Bloomington, IN 47405-7003. Phone: (812) 856-1925. Fax: (812) 856-5710. E-mail: azlotnic@indiana.edu.

[‡] University of Oklahoma Health Sciences Center.

[§] Present address: 250 McElroy Hall, Department of Veterinary Pathobiology, Oklahoma State University, Stillwater, OK 74078-2007.

[||] Indiana University.

[1] Abbreviations: HBV, hepatitis B virus; Cp, core protein; Cp149, 149-residue assembly domain of HBV Cp; EM, electron microscopy; SEC, size exclusion chromatography; *s*, statistical factor for reaction degeneracy; k_{nuc}, rate constant for nucleation; K_{assoc}, microscopic per subunit association constant.

10.1021/bi801814y CCC: $40.75
Published on Web 02/05/2009

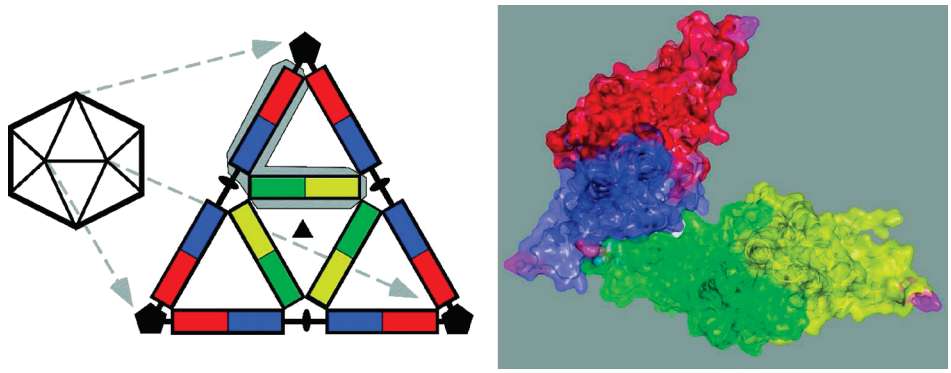

FIGURE 1: HBV capsids are composed of dimers that are held together by relatively small hydrophobic contacts. Capsids are icosahedral (far left) with each icosahedral facet (central panel) composed of two classes of dimer, AB (red and blue, respectively) and CD (yellow and green, respectively), that form the icosahedral asymmetric unit. A pair of dimers, highlighted in the central panel, are shown as translucent surfaces over a ribbon diagram. Residue Y132 (magenta) contributes to approximately 10% of the buried surface at each dimer−dimer interface.

this study, we develop an assembly deficient form of the HBV core protein as a model of an assembly-inhibited protein and investigate its effect on in vitro capsid assembly.

METHODS

Preparation and Purification of Cp149 and Cp149-Y132A. Cp149 was expressed in *Escherichia coli* from a pET11-based plasmid, pCp149, and purified using the detailed protocol described previously (*33*).

The Cp149-Y132A mutant was generated from pCp149 using a Quik-Change kit (Strategene). *E. coli* cells with the mutant plasmid were grown in LB broth with 50 μg/mL carbenicillin at 32 °C without induction. Cells suspended in the same lysis buffer used for the Cp149 purification (*33*) were lysed by sonication. Cell debris was removed by centrifugation for 50 min at 20000*g*. Protein was precipitated from the supernatant with 20% ammonium sulfate for 1 h followed by centrifugation for 50 min at 20000*g*. This pellet was resuspended in 20 mL of 100 mM Tris-HCl, 100 mM NaCl (pH 9.0), and 2 mM DTT, which was loaded onto a 5 cm × 70 cm column packed with Sephacryl S300 and equilibrated with resuspension buffer. Fractions were evaluated by SDS−PAGE and absorbance; Cp149-Y132A typically eluted at ~800 mL, consistent with a dimer rather than a capsid state. Pooled fractions were then adsorbed to a 5 mL Hi-Trap Q column, which was then washed with 5 column volumes of 50 mM Tris-HCl (pH 9.0), 80 mM NaCl, and 2 mM DTT (buffer QA). Samples were eluted with a gradient from 0 to 30% buffer QB (buffer QA with 2 M NaCl). Cp149-Y132A eluted at ~0.2 M NaCl. Fractions were pooled on the basis of SDS−PAGE and absorbance and then dialyzed into a storage buffer of 10 mM Tris-HCl (pH 9.0) and 2 mM DTT.

Light Scattering. Observations of kinetics by light scattering were performed as previously described (*23*). Briefly, scattering was observed with a Spex Flouromax 2 fluorometer set at 320 nm for both excitation and emission. Samples were in a black-masked microcuvette with a path length of 0.3 cm (Hellma). Initially, scattering was observed for a protein sample at twice the final concentration in buffer containing no NaCl, and then, after 10 s, buffer with twice the final NaCl concentration was manually added and mixed. Some samples were stored at a constant temperature, and the light scattering was read after 24 h. Light scattering is reported in arbitrary units.

Size Exclusion Chromatography (SEC). SEC was performed using a 21 mL Superose-6 column equilibrated with 0.1 M HEPES (pH 7.5) and either 0.15 or 1 M NaCl. The column was mounted on an AKTA-FPLC system recording absorbance at 280 nm. Peaks were quantified after manual baseline correction using the supplied Unicorn software (GE Health Sciences). Long-term kinetics were observed using a 21 mL Superose-6 column equilibrated with 50 mM HEPES (pH 7.5) and 1 M NaCl. The column was mounted on a Shimadzu-HPLC system equipped with an autoinjector to facilitate the long time course. Peaks at 280 nm were quantified after manual baseline correction using the supplied LCSolutions software (Shimadzu).

Electron Microscopy. Samples were adsorbed to glow-discharged carbon over paralodian copper grids (EM sciences). Samples were stained with 1−2% uranyl acetate and visualized with a Hitachi H7600 transmission electron microscope equipped with an AMT 2K × 2K CCD camera.

RESULTS

To model a capsid protein complexed with an assembly inhibitor, we designed an assembly deficient mutant. Interdimer contacts bury 1100−1400 Å^2 at the four quasi-equivalent interfaces (*17, 18*). In each case, tyrosine 132 contributes ~10% of the buried surface (*17, 18*). The phenolic side chain fits into a hydrophobic pocket formed by P20, D22, F23, F122, W125, A137, P138, I139, and L140A of a neighboring subunit. Similar contacts are made in a manner independent of quasi-equivalence. Mutation of Y132 to alanine is expected to decrease the amount of buried surface and also leave a destabilizing pocket (Figure 1).

The effect of the Y132A mutation was apparent during purification. Unlike Cp149, which is isolated from *E. coli* as a capsid, Cp149-Y132A was dimeric on the basis of size exclusion chromatography (SEC). The usual disassembly−reassembly purification of Cp149 (*33*) was necessarily abandoned and replaced with anion exchange chromatography (see Methods). The Y132A mutant retains the characteristic blue-shifted fluorescence spectrum of Cp149 and the helix-rich circular dichroism spectrum (data not shown) (*25*) and, as demonstrated in this paper, is capable of participating in assembly, all of which indicate that the mutant is properly

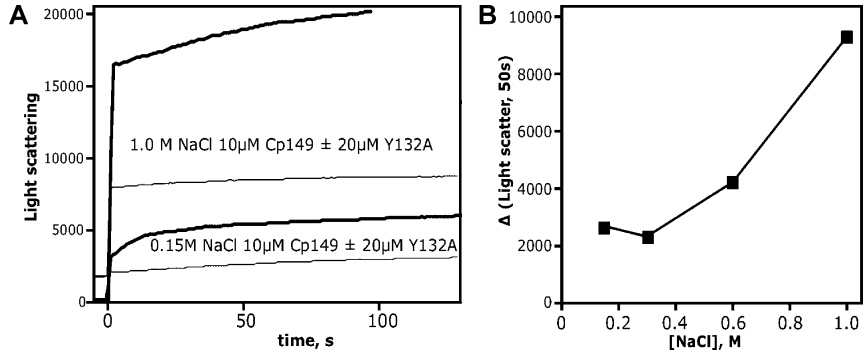

FIGURE 2: Cp149-Y132A coassembles with Cp149. (A) Representative kinetics of assembly at 37 °C observed by light scattering. Compared to control experiments of Cp149 without Cp149-Y123A (thin lines, offset for clarity), the presence of Cp149-Y132A leads to a great excess of light scatter. (B) Light scattering enhancement correlates with association energy, which is proportional to ionic strength; i.e., high ionic strength shows the greatest effect (*24*).

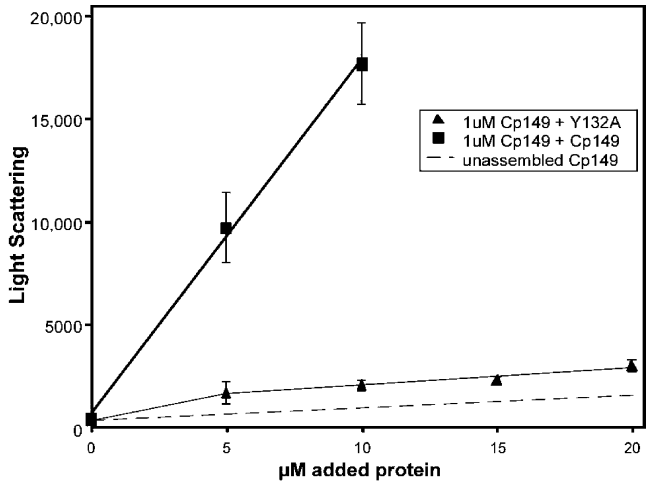

FIGURE 3: Coassembly is saturable. Samples containing 1 μM (final concentration) Cp149 and varying amounts of either Cp149 or Cp149-Y132A were induced to assemble at 21 °C by adding NaCl to a final concentration of 1 M. Light scattering was read after 24 h. Coassembly with Cp149-Y132A extrapolates to approximately twice the scattering of 1 μM Cp149. This enhanced light scattering indicates that Cp149 can only cooperate with a limited amount of mutant. Additional Cp149-Y132A does not poison coassembly. For comparison to the coassembly data, the scattering of corresponding concentrations of unassembled Cp149 is also shown (dashed line).

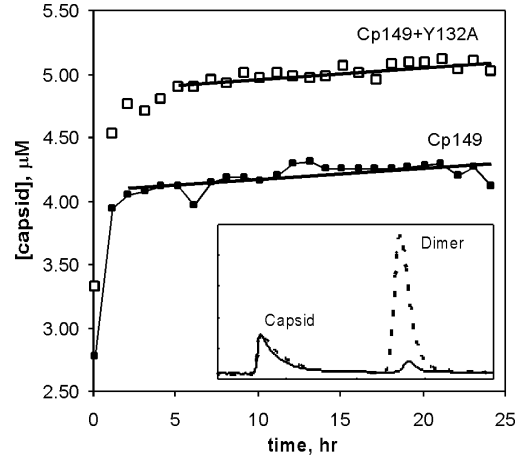

FIGURE 4: Comparing Cp149 assembly and Cp149-Y132A coassembly kinetics over 24 h. At long times, the rate of capsid formation is equal to, and thus diagnostic for, the rate of nucleation. SEC of 11.7 μM Cp149-Y132A coassembly with 5 μM wild type (□) results in more capsids than 5 μM Cp149 alone (■) but with a similar rate of assembly. The first point was taken 8 min postmixing and every hour thereafter. Assembly was induced by addition of NaCl to a final concentration of 0.6 mM in the presence of 1 mM DTT and eluted in 50 mM Hepes (pH 7.5) and 1.0 M NaCl. The inset shows overlaid SEC traces of Cp149 assembly (—) and Cp149-Y132A−Cp149 coassembly (---) at 23 h.

folded. Using light scattering, we found that purified Cp149-Y132A showed no sign of assembly at concentrations of 200 μM dimer in 1 M NaCl, conditions under which wild-type Cp149 has a pseudocritical concentration of <0.5 μM dimer (*23*).

We reasoned that Cp149-Y132A retained sufficient molecular complementarity that it could participate in assembly with wild-type Cp149. Initially, we used light scattering to examine the effect of varying association energy on coassembly (Figure 2). Cp149 assembly shows a strong correlation between ionic strength and the association constant (*24*). Coassembling 10 μM Cp149 with 20 μM Cp149-Y132A, we observed that there was additional light scattering compared to that with Cp149 alone. The kinetics of coassembly showed some peculiarities that were most evident under high-salt conditions. In 1 M NaCl, Cp149 alone assembles very rapidly, demonstrated by a very rapid increase in light scattering, faster than the dead time of manual mixing, followed by a near-horizontal plateau (Figure 2A). By comparison, the coassembly reaction shows a rapid rise followed by a continuing slow increase.

The light scatter enhancement was indeed correlated with ionic strength and, by extension, association constant (Figure 2B). Proportionally, the enhancement was always approximately 2-fold. However, it is the raw light scattering that correlates with the amount of Cp149 HBV assembly (*23*). Thus, these data suggest a substantial increase in the amount of assembly in the time course of this experiment.

As Cp149-Y132A coassembles with Cp149 but does not assemble on its own in HEPES and NaCl, we investigated whether there was a minimum proportion of Cp149 needed to nucleate assembly (Figure 3). For these experiments, we induced assembly of 1 μM Cp149 at 21 °C by addition of 1 M NaCl and observed the amount of light scattering at 24 h. For 1 μM Cp149, this should yield approximately 50% assembly; i.e., the pseudocritical concentration is approximately 0.5 μM. More importantly for this experiment, the high NaCl concentration was expected to lead to maximal

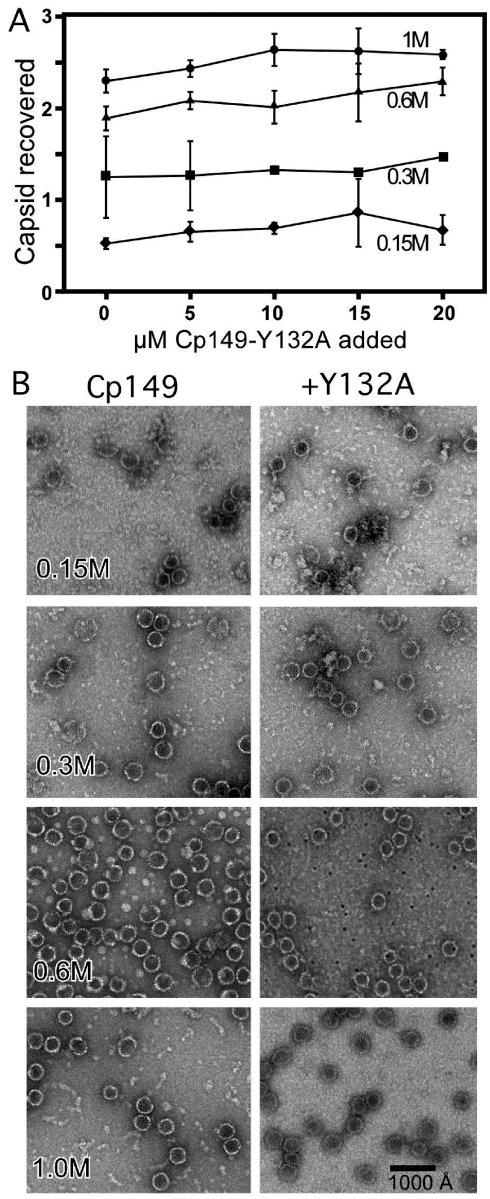

FIGURE 5: Coassembly of Cp149-Y132A with Cp149. (A) SEC under capsid stabilizing conditions shows that coassembly slightly increases the yield of capsids (2.5 units corresponds to ~8 μM dimer in the capsid peak). There is a weak but significant ($p < 0.02$) increase in the yield of capsid with an increased Y132A concentration for all but the 0.15 M NaCl experiments. Assembly with 10 μM Cp149 and a varying amount of mutant was carried out at 21 °C in 0.1 M HEPES (pH 7.5) with the stated NaCl concentration. After ~24 h, reaction mixtures were separated on a 21 mL Superose-6 column equilibrated with HEPES and 1 M NaCl. (B) Negatively stained electron micrographs of 24 h assembly reactions similar to those in panel A except these reactions included 20 μM Cp149-Y132A.

participation of Cp149-Y132A. Control reactions, in which more Cp149 was added to the basal concentration of 1 μM and then induced to assemble, showed the expected linear increase in scattering consistent with assembly of all protein in excess of the pseudocritical concentration (*21, 24*). Addition of Cp149-Y132A increased the light scattering by approximately 2-fold, after accounting for the scattering of free dimer, in good agreement with the results shown in Figure 2. Higher proportions of mutant did not generate any further excess of light scattering, suggesting that a large proportion of the capsid was wild-type Cp149. We also noted

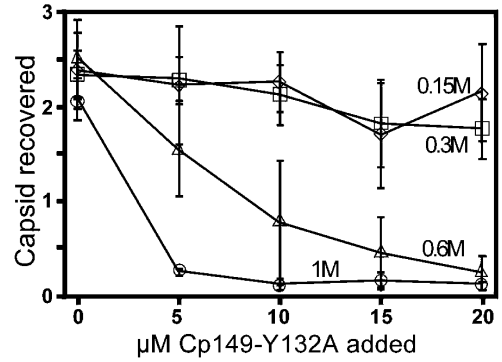

FIGURE 6: Coassembly of Cp149-Y132A with Cp149 results in fragile capsids. These experiments are similar to those shown in Figure 5A except reaction mixtures were incubated at 37 °C, resulting in ≥80% assembly at all ionic strengths. To examine particle stability, SEC was performed on a Superose-6 column equilibrated in HEPES buffer with only 0.15 M NaCl, an ionic strength at which capsids are nominally stable.

that high concentrations of Cp149-Y132A did not decrease light scattering, suggesting that the mutant did not poison assembly.

To further investigate the effects of Cp149-Y132A on assembly, we examined the long-term kinetics of assembly over a 24 h period. In capsid assembly reactions, after the initial burst of assembly, a steady state of intermediates is generated and the nucleation rate is equal to the rate of capsid formation (*21, 22*). For formation of the trimer of dimer nucleus of HBV (*23*)

$$d[\text{capsid}]/dt = [\text{nucleus}]/dt = sk_{\text{nuc}}K_{\text{assoc}}[\text{Cp}]^3 \qquad (1)$$

where k_{nuc} is the microscopic nucleation rate constant in M^{-1} s^{-1}, s is a statistical factor, K_{assoc} (M^{-1}) is the association constant for pairwise interaction between dimers, and [Cp] is the concentration of free dimer. A coassembly reaction of 11.7 μM Cp149-Y132A with 5 μM wild-type protein at 0.6 M NaCl was monitored by SEC over a 24 h equilibration period and compared to a control experiment with 5 μM wild-type Cp149 (Figure 4). As the reaction approached equilibrium, the coassembly reaction yielded roughly 20% more capsid. The slopes of the steady state portion of the reaction, d[capsid]/dt, between 5 and 20 h, are approximately identical between the coassembly and the wild-type-only assembly. However, the coassembly takes substantially longer to reach this steady state.

We examined assembly products by size exclusion chromatography (SEC) and electron microscopy (EM). Initially, SEC was performed using a column equilibrated in 1 M NaCl to stabilize coassembled capsids (Figure 5A). Samples with 10 μM Cp149 and varying concentrations of mutant and NaCl were incubated overnight before separation of capsid and dimer by SEC. As the concentration of Cp149-Y132A was increased, we observed small but significant ($p < 0.02$) increases in the yield of capsid for 0.3, 0.6, and 1.0 M NaCl reactions, though not the great excess suggested by light scattering. The minimal increase in assembly led us to question whether the mutant was actually contributing to capsid formation or if the excess light scattering represented some capsid-associated aggregation.

To test this possibility, we examined coassembly reactions using SEC columns equilibrated in a lower-ionic strength buffer, 0.15 M NaCl (Figure 6). Normal Cp149 capsids

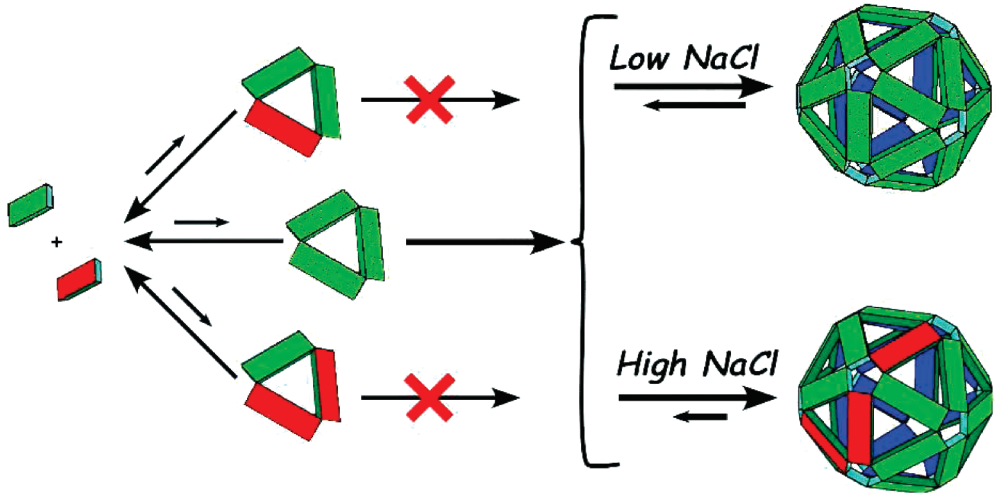

FIGURE 7: Model describing the roles that Cp149-Y132 plays in assembly. The mutant cannot nucleate assembly on its own. The relatively slow assembly that takes place in the presence of excess mutant suggests that it can play a slight role in retarding nucleation. When association energy between subunits is weak (low NaCl concentrations), incorporated subunits dissociate during assembly to yield capsids that are enriched in wild type. When association is strong (high NaCl concentrations), the mutant is retained in capsids with the long-term effect that these capsids readily dissociate, as shown in Figure 6. Assembly inhibitors and defective subunits are expected to fill similar roles.

persist in mildly destabilizing environments of low salt and low concentration due to hysteresis to dissociation (*25*). In these experiments, we used reactions similar to those shown in Figure 5 except that reaction mixtures were incubated at 37 °C where the level of association is greater. Coassembly reactions induced by 0.15 and 0.3 M NaCl showed no significant change in the yield of capsid related to Cp149-Y132A, essentially the same result found when the column was equilibrated with 1 M NaCl buffer. However, coassembly reactions induced by high salt, 0.6 and 1 M NaCl, showed dramatically different results. When these high-NaCl concentration reaction mixtures were injected onto a SEC column equilibrated with a low concentration of NaCl, we observed a dose-dependent decrease in the yield of assembled particles. By comparison, recovery of capsids from high-salt assembly reactions using pure Cp149 is nearly quantitative. The difference between results for low- and high-ionic strength SEC indicates the participation of the Y132A mutant in assembly and its sensitivity to association energy.

To define the morphology of the products from coassembly reactions, samples equilibrated for 24 h were visualized by negative stain electron microscopy (Figure 5b). At all NaCl concentrations, coassembled particles appeared essentially the same as those with wild-type protein alone. Micrographs of coassembly reactions are almost indistinguishable from those of Cp149 reactions except for the background attributable to high concentrations of free protein, in this case Cp149-Y132A. These micrographs are for samples assembled at 21 °C, but the same result was observed in reaction mixtures incubated at 37 °C (data not shown).

DISCUSSION

On the basis of structure, we developed a point mutation within the HBV core protein, Cp149-Y132A, as a tool for examining the process of assembly inhibition. We have shown that this mutant is deficient in assembly but is capable of coassembling with wild-type Cp149. The extent of coassembly appears to be increased by high ionic strength, which increases the protein−protein association energy of HBV core protein (*24*). The critical observation for confirming coassembly was that high-salt reactions generated capsids that were unusually fragile as demonstrated by their dissociation during SEC under conditions where the pseudocritical concentration of Cp149 is ~5 μM but Cp149 capsids persist due to hysteresis (*25*).

These results can be interpreted in terms of a broad framework of nucleated assembly based on a network of weak interactions (Figure 7), typical for most viruses (*34, 35*). On the basis of structure, it is reasonable to posit that Cp149-Y132A has a substantially weaker association energy. Cp149-Y132A appears to be incapable of nucleating assembly. At high salt concentrations, which strengthen association energy, it may competitively inhibit nucleation by transiently binding to nucleation competent Cp149. This is consistent with the kinetic effect most obvious under high-salt conditions in Figures 2A and 4. The mutant participates in assembly when there is both strong and weak association energy. However, with weak association energy, mutant subunits (analogous to defective subunits or inhibitor-bound subunits) are thermodynamically edited from the growing capsid.

We examined the effect of Cp149-Y132A on nucleation rate in a long-term kinetics experiment. On the basis of model studies, assembly reactions rapidly achieve a steady state of intermediates where the rate of capsid formation is equal to the rate of nucleation; thus, the rate of capsid production is a direct readout of the nucleation rate (*21, 22*). Quantitative interpretation of coassembly is complicated by the presence of two species of subunit with different association energies, rate constants, and concentrations that vary in ill-defined ways. However, the data suggest limiting models of the role of Cp149-Y132A. In Figure 4, it is apparent that the rate of capsid formation is essentially unchanged by the presence of Cp149-Y132A, although the yield is increased. One explanation for the unchanged reaction rate is that the mutant does not participate in nucleation, the rate-limiting step of capsid assembly. In this scenario, the rate of nucleus

formation is determined solely by the wild-type Cp149 and Cp149-Y132A participates only in "elongation" of intermediates, hence the greater yield of capsid. It is the weaker association energy of the mutant that leads to the slower establishment of the steady state.

An alternative explanation is that Cp149-Y132A participates in assembly so poorly that it competitively inhibits nucleation but is incorporated during elongation. Nuclei and prenuclear intermediates formed with the weakly associating mutant would have a stronger tendency to dissociate rather than elongate. Thus, wild-type protein would be tied up unproductively. The resulting attenuation of nucleation would be partially compensated by the high concentration of mutant. The expected effect would be the apparent lag in reaching the steady state, as observed.

The behavior of capsids is straightforward. SEC with the column equilibrated with a low salt concentration shows distinct differences in the stability of coassembly products formed at low versus high NaCl concentrations. At lower NaCl concentrations, weakly associated proteins have a chance to be thermodynamically edited from growing and completed capsids; i.e., defective proteins will be preferentially excluded in a stochastic equilibrium. Thus, at lower NaCl concentrations, there is no change in the yield of capsid. At higher NaCl concentrations, with stronger association energy, Cp149-Y132A is retained in capsids resulting in unstable capsids that dissociate in low-NaCl concentration SEC. Apparently, even a small amount of Cp149-Y132A was sufficient to compromise capsid stability. It appears that only a limited amount of Y132A can be incorporated into capsids (Figure 3), because it either does not bind or is edited away. Two possible explanations arise for this result: (i) a patch of defective protein is too unstable to be retained, or (ii) Y132A promotes a quaternary structure change, weakening binding sites some distance from the defect, that limits association with the wild type.

The balance between capsid stability and lability is critical to biological function (e.g., ref *36*). A number of mutants accumulate in chronic HBV that appear to subtly enhance (*37*−*40*) and in a compensatory manner attenuate assembly (*41*−*43*). However, the effect of Y132A in Cp149 is unsubtle. Even in the full-length core protein, where assembly is supported by interaction with nucleic acid, evidence suggests that the Y132A mutation prevents assembly in bacterial (*13*) and mammalian expression systems (*44*). Evidence suggests that the Y132A mutation prevents assembly of the full-length core protein, even though the capsid is also stabilized by interaction with packaged nucleic acid.

Our results have implications for the development of antiviral approaches that target assembly (*29*) and for control of self-assembling systems in nanotechnology (*3*). For an antiviral assembly inhibitor that prevents a bound subunit from assembling or where weak interactions readily allow editing of inhibitor-bound subunits, there will need to be greater than stoichiometric concentrations of inhibitor in a cell. In short, preventing assembly altogether is likely to be an unsuccessful strategy. On the other hand, an inhibitor that participates in assembly to poison the reaction or to generate fragile capsids can be effective at substoichiometric ratios. At low NaCl concentrations, Cp149-Y132A does not stay included in capsids and thus mimics the effects of a protein with a tightly bound inhibitor that altogether prevents assembly. At high NaCl concentrations, Cp149-Y132A participates in assembly to generate fragile capsids but does not poison assembly in a crystallographic sense by blocking further growth. These diverse activities may be ideal for distinct critical roles in regulating formation of self-assembling nanostructures. It is easy to picture roles for labile inhibitors in preventing inopportune assembly or acting as protecting groups to block assembly. Identification of small molecules and mutants that regulate assembly remains an ongoing area of research.

ACKNOWLEDGMENT

We are indebted to Drs. Steven Stahl and Paul Wingfield for their preliminary studies with assembly deficient Cp149 mutants and to Jennifer M. Johnson for comments and technical assistance. Electron microscopy was performed at the Oklahoma Medical Research Foundation imaging core facility.

REFERENCES

1. Fields, B. N., Knipe, D. M., Howley, P. M., Chanock, R. M., Melnick, J. L., Monath, T. P., Roizman, B., and Straus, S. E. (1996) *Virology*, 3rd ed., Lippincott-Raven Publishers, Philadelphia.
2. Douglas, T., and Young, M. (1998) Host-guest encapsulation of materials by assembled virus protein cages. *Nature 393*, 152–155.
3. Douglas, T., and Young, M. (2006) Viruses: Making friends with old foes. *Science 312*, 873–875.
4. Wang, Q., Lin, T., Tang, L., Johnson, J. E., and Finn, M. G. (2002) Icosahedral virus particles as addressable nanoscale building blocks. *Angew. Chem., Int. Ed. 41*, 459–462.
5. Falkner, J. C., Turner, M. E., Bosworth, J. K., Trentler, T. J., Johnson, J. E., Lin, T., and Colvin, V. L. (2005) Virus crystals as nanocomposite scaffolds. *J. Am. Chem. Soc. 127*, 5274–5275.
6. Chen, C., Daniel, M. C., Quinkert, Z. T., De, M., Stein, B., Bowman, V. D., Chipman, P. R., Rotello, V. M., Kao, C. C., and Dragnea, B. (2006) Nanoparticle-templated assembly of viral protein cages. *Nano Lett. 6*, 611–615.
7. Sun, J., DuFort, C., Daniel, M. C., Murali, A., Chen, C., Gopinath, K., Stein, B., De, M., Rotello, V. M., Holzenburg, A., Kao, C. C., and Dragnea, B. (2007) Core-controlled polymorphism in virus-like particles. *Proc. Natl. Acad. Sci. U.S.A. 104*, 1354–1359.
8. Mukherjee, S., Pfeifer, C. M., Johnson, J. M., Liu, J., and Zlotnick, A. (2006) Redirecting the coat protein of a spherical virus to assemble into tubular nanostructures. *J. Am. Chem. Soc. 128*, 2538–2539.
9. Ganem, D., and Schneider, R. J. (2001) *Hepadnaviridae: The Viruses and Their Replication*, 4th ed., Lippincott Williams & Wilkins, Philadelphia.
10. Crowther, R. A., Kiselev, N. A., Bottcher, B., Berriman, J. A., Borisova, G. P., Ose, V., and Pumpens, P. (1994) Three-dimensional structure of hepatitis B virus core particles determined by electron cryomicroscopy. *Cell 77*, 943–950.
11. Zlotnick, A., Cheng, N., Conway, J. F., Booy, F. P., Steven, A. C., Stahl, S. J., and Wingfield, P. T. (1996) Dimorphism of hepatitis B virus capsids is strongly influenced by the C-terminus of the capsid protein. *Biochemistry 35*, 7412–7421.
12. Seeger, C., and Mason, W. S. (2000) Hepatitis B virus biology. *Microbiol. Mol. Biol. Rev. 64*, 51–68.
13. Koschel, M., Thomssen, R., and Bruss, V. (1999) Extensive mutagenesis of the hepatitis B virus core gene and mapping of mutations that allow capsid formation. *J. Virol. 73*, 2153–2160.
14. Koschel, M., Oed, D., Gerelsaikhan, T., Thomssen, R., and Bruss, V. (2000) Hepatitis B virus core gene mutations which block nucleocapsid envelopment. *J. Virol. 74*, 1–7.
15. Ponsel, D., and Bruss, V. (2003) Mapping of amino acid side chains on the surface of hepatitis B virus capsids required for envelopment and virion formation. *J. Virol. 77*, 416–422.
16. Birnbaum, F., and Nassal, M. (1990) Hepatitis B virus nucleocapsid assembly: Primary structure requirements in the core protein. *J. Virol. 64*, 3319–3330.

17. Wynne, S. A., Crowther, R. A., and Leslie, A. G. (1999) The crystal structure of the human hepatitis B virus capsid. *Mol. Cell 3*, 771–780.
18. Bourne, C., Finn, M. G., and Zlotnick, A. (2006) Global structural changes in hepatitis B capsids induced by the assembly effector HAP1. *J. Virol. 80*, 11055–11061.
19. Stray, S. J., Bourne, C. R., Punna, S., Lewis, W. G., Finn, M. G., and Zlotnick, A. (2005) A heteroaryldihydropyrimidine activates and can misdirect hepatitis B virus capsid assembly. *Proc. Natl. Acad. Sci. U.S.A. 102*, 8138–8143.
20. Bourne, C., Lee, S., Venkataiah, B., Lee, A., Korba, B., Finn, M. G., and Zlotnick, A. (2008) Small-Molecule Effectors of Hepatitis B Virus Capsid Assembly Give Insight into Virus Life Cycle. *J. Virol. 82*, 10262–10270.
21. Zlotnick, A. (1994) To build a virus capsid. An equilibrium model of the self assembly of polyhedral protein complexes. *J. Mol. Biol. 241*, 59–67.
22. Endres, D., and Zlotnick, A. (2002) Model-based Analysis of Assembly Kinetics for Virus Capsids or Other Spherical Polymers. *Biophys. J. 83*, 1217–1230.
23. Zlotnick, A., Johnson, J. M., Wingfield, P. W., Stahl, S. J., and Endres, D. (1999) A theoretical model successfully identifies features of hepatitis B virus capsid assembly. *Biochemistry 38*, 14644–14652.
24. Ceres, P., and Zlotnick, A. (2002) Weak protein-protein interactions are sufficient to drive assembly of hepatitis B virus capsids. *Biochemistry 41*, 11525–11531.
25. Singh, S., and Zlotnick, A. (2003) Observed hysteresis of virus capsid disassembly is implicit in kinetic models of assembly. *J. Biol. Chem. 278*, 18249–18255.
26. Vogel, M., Diez, M., Eisfeld, J., and Nassal, M. (2005) In vitro assembly of mosaic hepatitis B virus capsid-like particles (CLPs): Rescue into CLPs of assembly-deficient core protein fusions and FRET-suited CLPs. *FEBS Lett. 579*, 5211–5216.
27. Stray, S. J., and Zlotnick, A. (2006) BAY 41-4109 has multiple effects on Hepatitis B virus capsid assembly. *J. Mol. Recognit. 19*, 542–548.
28. Prevelige, P. E. J. (1998) Inhibiting virus-capsid assembly by altering the polymerisation pathway. *Trends Biotechnol. 16*, 61–65.
29. Zlotnick, A., Ceres, P., Singh, S., and Johnson, J. M. (2002) A small molecule inhibits and misdirects assembly of hepatitis B virus capsids. *J. Virol. 76*, 4848–4854.
30. Teschke, C. M., King, J., and Prevelige, P. E., Jr. (1993) Inhibition of viral capsid assembly by 1,1′-bi(4-anilinonaphthalene-5-sulfonic acid). *Biochemistry 32*, 10658–10665.
31. Sticht, J., Humbert, M., Findlow, S., Bodem, J., Muller, B., Dietrich, U., Werner, J., and Krausslich, H. G. (2005) A peptide inhibitor of HIV-1 assembly in vitro. *Nat. Struct. Mol. Biol. 12*, 671–677.
32. Vogt, V. M. (2005) Blocking HIV-1 virus assembly. *Nat. Struct. Mol. Biol. 12*, 638–639.
33. Zlotnick, A., Lee, A., Bourne, C. R., Johnson, J. M., Domanico, P. L., and Stray, S. J. (2007) In vitro screening for molecules that affect virus capsid assembly (and other protein association reactions). *Nat. Protoc. 2*, 490–498.
34. Zlotnick, A. (2005) Theoretical aspects of virus capsid assembly. *J. Mol. Recognit. 18*, 479–490.
35. Zlotnick, A. (2003) Are weak protein-protein interactions the general rule in capsid assembly? *Virology 315*, 269–274.
36. Forshey, B. M., von Schwedler, U., Sundquist, W. I., and Aiken, C. (2002) Formation of a human immunodeficiency virus type 1 core of optimal stability is crucial for viral replication. *J. Virol. 76*, 5667–5677.
37. Yuan, T. T., Sahu, G. K., Whitehead, W. E., Greenberg, R., and Shih, C. (1999) The mechanism of an immature secretion phenotype of a highly frequent naturally occurring missense mutation at codon 97 of human hepatitis B virus core antigen. *J. Virol. 73*, 5731–5740.
38. Yuan, T. T., Tai, P. C., and Shih, C. (1999) Subtype-independent immature secretion and subtype-dependent replication deficiency of a highly frequent, naturally occurring mutation of human hepatitis B virus core antigen. *J. Virol. 73*, 10122–10128.
39. Suk, F. M., Lin, M. H., Newman, M., Pan, S., Chen, S. H., Liu, J. D., and Shih, C. (2002) Replication advantage and host factor-independent phenotypes attributable to a common naturally occurring capsid mutation (I97L) in human hepatitis B virus. *J. Virol. 76*, 12069–12077.
40. Ceres, P., Stray, S. J., and Zlotnick, A. (2004) Hepatitis B Virus Capsid Assembly is Enhanced by Naturally Occurring Mutation F97L. *J. Virol. 78*, 9538–9543.
41. Le Pogam, S., Yuan, T. T., Sahu, G. K., Chatterjee, S., and Shih, C. (2000) Low-level secretion of human hepatitis B virus virions caused by two independent, naturally occurring mutations (P5T and L60V) in the capsid protein. *J. Virol. 74*, 9099–9105.
42. Yuan, T. T., and Shih, C. (2000) A frequent, naturally occurring mutation (P130T) of human hepatitis B virus core antigen is compensatory for immature secretion phenotype of another frequent variant (I97L). *J. Virol. 74*, 4929–4932.
43. Chua, P. K., Wen, Y. M., and Shih, C. (2003) Coexistence of two distinct secretion mutations (P5T and I97L) in hepatitis B virus core produces a wild-type pattern of secretion. *J. Virol. 77*, 7673–7676.
44. Rost, M., Mann, S., Lambert, C., Doring, T., Thome, N., and Prange, R. (2006) Gamma-adaptin, a novel ubiquitin-interacting adaptor, and Nedd4 ubiquitin ligase control hepatitis B virus maturation. *J. Biol. Chem. 281*, 29297–29308.

BI801814Y